Experimental Results of Passive SAR Imaging Using DVB-T Illuminators of Opportunity

Damian Gromek, *Student Member, IEEE*, Krzysztof Kulpa, *Senior Member, IEEE*, and Piotr Samczyński, *Senior Member, IEEE*

***Abstract*—In this letter, pioneering experimental results of passive synthetic aperture radar (SAR) imaging are presented. The classical active SAR radar operates in monostatic geometry. The SAR sensor presented in this letter is a passive radar utilizing commercial Digital Video Broadcasting—Terrestrial transmitters as illuminators of opportunity. It works in a bistatic configuration, where the receiver is placed on a moving platform and the transmitter is placed on the ground and is stationary. The imaged scenes are stationary surfaces on Earth such as agriculture or urban areas, buildings, etc. In this letter, pioneering results of signal processing verified by a measurement campaign are presented. In the experiment, two synchronized passive radar receivers were mounted on a small airborne platform. The main goal of the presented experiment was to verify the possibility of ground imaging using passive SAR technology and validate previously presented theoretical results.**

***Index Terms*—Bistatic SAR (BSAR), Digital Video Broadcasting—Terrestrial (DVB-T), passive radar, passive SAR, synthetic aperture radar (SAR).**

I. Introduction

ONE of the most popular methods for Earth surface imaging is the synthetic aperture radar (SAR) technique. It was proposed for the first time in 1951 by Carl Willey from the Goodyear Aircraft Corporation [1], [2]. Since that time, SAR has been intensively developed, and many new concepts of image creation have been proposed [3], [4]. Nowadays, SAR imaging has entered a stage of technological maturity and is widely used in sensors mounted on different kinds of moving platforms such as satellites, aircraft, and unmanned aerial vehicles. Most of the SAR techniques are based on monostatic technology, where both transmitter and receiver are onboard the same air- or spaceborne platform. In the last two decades, intensive studies have been carried out on bistatic and multistatic radar observation, including testing of the bistatic SAR concept [5], [6]. The main feature of the bistatic radar system is the physical separation between the transmitter and the receiver. The main advantage of such a configuration is that a target can be observed from different bistatic angles, providing more information about the target. A further step in bistatic radar development is to use transmitters of opportunity for scene illumination instead of dedicated and easily detected SAR transmitters. This leads directly to the idea of passive SAR imaging.

Passive radar is a technology which has been known for over 70 years due to the radar experiment conducted by Arnold Wilkins and Robert Watson-Watt in Daventry, U.K. Passive technology was sidelined for many years afterward as it was too difficult to implement using analog circuits. Nowadays, in the age of digital signal processing, passive technology is being rediscovered [7]–[13]. This technology allows existing emissions (e.g., FM radio, GSM, analog TV, Digital Video Broadcasting—Terrestrial (DVB-T), and DVB-S, among others) to be used for object detection. One of the fundamental advantages of passive technology is the difficulty in detecting a passive radar as it does not emit electromagnetic energy. As a result, it does not need a spectrum allocation, so it can be considered "green" technology, which is safe for the environment.

The concept presented in this letter is based on the three technologies mentioned previously. It combines SAR, bistatic radar, and passive radar technology using ground-based transmitters of opportunity for illumination. The best candidate from all of the available ground-based commercial illuminators (FM-radio, DVB-T, and GSM, among others) for passive SAR imaging purposes seems to be the DVB-T transmitter. This is due to its relatively high power (10–100 kW), which provides a good power budget and a reasonable bandwidth (ca. 7.6 MHz for single DVB-T channel), giving a fine resolution of up to 20 m [16], [21], [22]. In many places, it is possible to find the illumination of a wider bandwidth, while multiple channels are often transmitted from the same place. This leads to the improvement of the range resolution of the passive SAR.

In the literature, one can find descriptions of such concepts [14]–[16], but up to now, only two preliminary results of experimental trials have been published in open literature. In [16], the authors present a range-Doppler map of the observed ground area obtained using a DVB-T-based passive radar. Such a method is similar to unfocused SAR processing. In [12] are the results of a single-channel passive SAR processing obtained from a CARABAS SAR system working in passive mode.

In this letter, the authors present recent experimental results obtained using a DVB-T-based passive SAR demonstrator equipped with two synchronous receiving channels: one channel used for direct (reference) signal acquisition and the second (surveillance) for ground echo signal. The two-channel solution increases the dynamics of the final passive SAR image and reduces the direct signal masking effect [15], [18].

Manuscript received December 11, 2015; revised May 5, 2016; accepted May 18, 2016. Date of publication June 15, 2016; date of current version July 20, 2016.

The authors are with the Institute of Electronic Systems, Warsaw University of Technology, 00-665 Warsaw, Poland (e-mail: dgromek@elka.pw.edu.pl).

Color versions of one or more of the figures in this paper are available online at http://ieeexplore.ieee.org.

Digital Object Identifier 10.1109/LGRS.2016.2571901

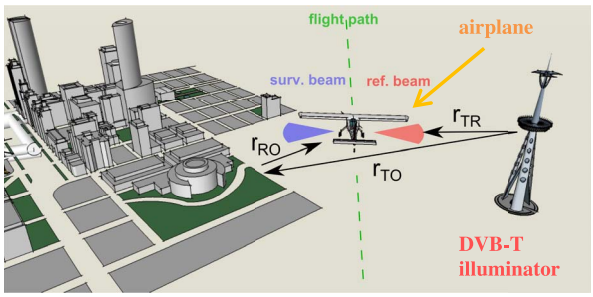

Fig. 1. Simplified passive SAR scenario.

II. Concept of Passive SAR Imaging

The considered passive SAR system consists of a radar receiver mounted on a mobile airborne platform which utilizes a transmitter of opportunity.

The typical system geometry is presented in Fig. 1. In this letter, the quasi-monostatic scenario is analyzed (the bistatic angle is close to zero). This means that the observation angle of the target by the radar is close to the angle of incidence of radiation from the transmitter. The other assumption is that the airborne radar receiver is travelling between the source of illumination and the imaged target, so it is possible to place reference and surveillance antennas on opposite sides of the airplane's fuselage.

In the passive radar concept, synchronization is required between the two receiving channels since range profiles are obtained by the computation of the cross-correlation or cross-ambiguity functions between the reference and surveillance signals. Synchronization between the passive SAR receiver and the DVB-T transmitter is not required.

In the concept presented, the passive radar is equipped with two antennas mounted on opposite sides of the airborne platform. The reference antenna is directed toward the transmitter, and the surveillance one is directed toward the imaged area. As a result, the radar platform trajectory should be between the transmitter and the imaged area.

As both antennas receive the direct signal and surveillance signal simultaneously, the requirement for the dynamic range of a single-channel passive radar receiver is very high—at least 100 dB. A typical active radar dynamic range is 50–70 dB. In the case where a two-channel passive radar is used with separate reference and surveillance antennas, the direct signal to echo signal ratio is decreased by the antenna separation factor. Due to this isolation, which, in practice, is at the level of 20–30 dB, the direct signal to echo signal ratio in the surveillance channel is limited to 60–90 dB, which can be handled by modern AD converters. The remaining direct power, which can still mask the weak signals, can be further removed using CLEAN techniques [18], [19]. The application of this procedure reduces the direct signal by 20–60 dB, which significantly decreases the masking effect and improves the final passive SAR image.

The signal received by the antennas can be described as a sum of the direct signal and echo signals

$$S_{\substack{\text{ref}\\\text{sur}}}(t) = As_T\left(t - t_{\text{TR}}(t)\right) + \sum_k A_k s_T\left(t - t_{\text{TO},k} - t_{\text{RO},k}(t)\right) + \xi(t) \quad (1)$$

where

A/A_k	amplitudes of the direct/reflected echo signals;
$S_T(t)$	DVB-T continuous wave illuminating signal;
$t_{\text{TR}}(t)$	time delay related to distance between moving radar receiver and stationary DVB-T illuminator $= (r(t)_{\text{TR}}/c)$);
$t_{\text{TO},k}$	time delay related to distance between kth target and stationary DVB-T illuminator $= (r_{\text{TO},k}/c)$;
$t_{\text{RO},k}(t)$	time delay related to distance between kth target and moving airborne radar receiver $= (r(t)_{\text{RO},k}/c)$;
$\xi(t)$	Gaussian additive noise.

Naturally, the detection is based on finding the time and Doppler shifted copies of the illuminating signal in the echo. The processing is done using the cross-correlation between the reference and surveillance signals. The DVB-T signal is treated here as a narrowband noise waveform signal. The cross-correlation function produces range profiles according to the following equation:

$$s_{\text{corr}}(i,\tau) = \int s_{\text{sur}}(i,t)s^*_{\text{ref}}(i,t-\tau)dt \quad (2)$$

where

$S_{\text{ref}}(i)$	ith block of reference DVB-T signal;
$S_{\text{sur}}(i)$	ith block of surveillance DVB-T signal;
$S_{\text{corr}}(i)$	ith range profile.

Due to the movement of the passive radar receiver, different ground objects produce different Doppler frequencies in the azimuthal direction. The authors have presented the analysis of the range migration and Doppler history for ground targets in [24]. As a result, matched filtration in the azimuthal direction produces a focused passive SAR image. From the knowledge of the position of the transmitter and the trajectory of the passive radar, the position of a ground-based stationary target can also be determined. The final SAR image can be obtained by applying the back-projection algorithm on the artificially created matrix of raw data. In the back-projection algorithm, the final SAR image is obtained by calculating each pixel according to the equation

$$\text{SAR}(x,y) = \int s_{\text{corr}}\left(i, t_{(x,y)}(i)\right) * e^{-j\varphi_{(x,y)}(i)}di \quad (3)$$

where

$$t_{(x,y)}(i) = \frac{r_{B(x,y)}(i)}{c} \quad (4)$$

$$\varphi_{(x,y)}(i) = \frac{2\pi}{\lambda}r_{B(x,y)}(i) \quad (5)$$

$$r_{B(x,y)}(i) = r_{\text{TO}(x,y)} + r_{\text{RO}(x,y)}(i) - r_{\text{TR}}(i).$$

The $t_{(x,y)}(i)$ is the time delay of the echo in the ith artificially created pulse $s_{(\text{corr})}(i)$ from the point scatterer placed on the flat ground scene at coordinates (x,y), and the $\varphi_{(x,y)}(i)$ represents the signal phase for that single scatterer. The time

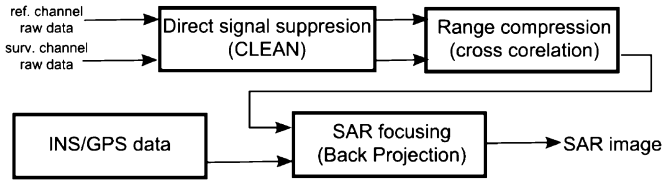

Fig. 2. Signal processing chain.

delay $t_{(x,y)}(i)$ and signal phase $\varphi_{(x,y)}(i)$ are determined by the bistatic distance $r_{B(x,y)}(i)$.

III. Signal Processing Chain for DVB-T Passive SAR Imaging

The final passive SAR image is created by a digital SAR processor. The signal processing chain for an airborne passive SAR is presented in Fig. 2. The whole DVB-T signal structure—the pilot signals and guard intervals—is kept in the signal processing algorithm proposed by the authors. The DVB-T signal is treated in the proposed algorithm as a narrowband noise signal.

The first step of the signal processing is the adaptive cancelation of the strong direct echo, which has to be removed from the surveillance channel. In order to do this, each signal (reference and surveillance) is divided into small blocks (each block of a few millisecond duration—in this case 1 ms), and then, the direct echo signal is removed from the surveillance channel in each block. This operation is done using adaptive filtering. There are two types of adaptive filters: recursive and block based. The authors of this letter decided to use the second type since it can be efficiently implemented in hardware and software. For these purposes, the authors chose the CLEAN algorithm [18], [19], commonly used in PCL processing.

The second step is range compression. For this purpose, the cross-correlation function is calculated between the reference and filtered surveillance signals. After this step, a 2-D data matrix is formed in the range (fast time) and slow time domain.

The final step is the cross-range compression. For a short observation time, when the range migration can be neglected, azimuth compression can be obtained by applying FFT along the azimuth–slow time direction, which was shown in [16]. For a longer integration time, the range migration correction and matched filtration algorithms are required to obtain a focused SAR image. A SAR image can be obtained using the back-projection algorithm [20]. The back-projection algorithm includes both compensation of range migration and matched filtration in the azimuth direction and can be relatively easily adopted for passive SAR imaging.

In the following chapter, real results of passive SAR imagery based on DVB-T illumination will be shown. The final results of signal processing will be shown in the next paragraph.

IV. In-Flight Measurement Campaign

The measurement campaign took place in December 2014. Measurements were made in the city of Sierpc, Poland, near which a DVB-T transmitter was located. The DVB-T illuminator of opportunity GPS coordinates are 52.89° N, 19.65° E.

Fig. 3. Airborne passive radar receiver.

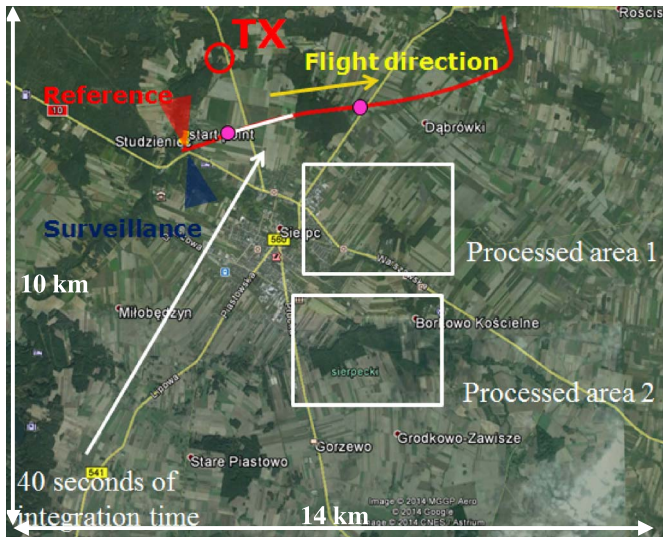

Fig. 4. Measurement scenario.

The DVB-T carrier frequency used in the experiment was 618 MHz, with an EIRP of 100 kW. The transmitter mast height was 250 m above ground level. The Polish plane PZL-104 "Wilga" was used as a mobile platform, on which a passive receiver was mounted (see Fig. 3).

The passive radar demonstrator was constructed using COTS—Commercial Off The Shelf elements including DVB-T antennas, a USRP N210 as a data acquisition unit, and a portable PC for data recording and processing, as depicted in Fig. 3.

The measurement scenario is presented in Fig. 4. The red line represents the flight path given by the GPS/INS device. The speed of the platform during the flight was around 40 m/s. The altitude of the aircraft was around 300 m above the ground. The total traveled distance, shown in Fig. 4, was around 8 km (200 s × 40 m/s). The shortest distance between the flight path and the transmitter was c.a. 2 km. In Fig. 4, areas which were processed using a back-projection algorithm in order to obtain SAR images are also marked. The single pixel size of the image

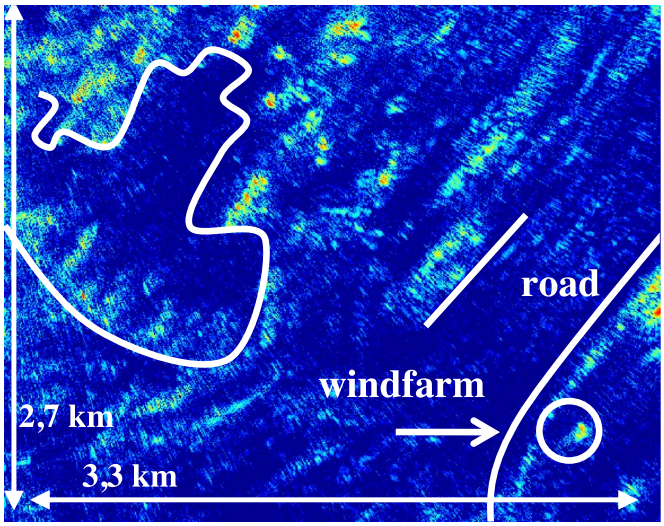

Fig. 5. Passive SAR image of area No. 1 (see Fig. 4).

Fig. 6. Google optical image of area No. 1 (see Fig. 4).

in the back-projection algorithm was 3 m × 3 m. The integration time in azimuth in this case was 40 s (which is around 1.6 km of synthetic aperture), and the integration path is marked with a white line in Fig. 4. The authors relied on the INS/GPS data provided by the equipment, and no additional motion compensation technique was applied in signal processing. The INS/GPS device provided the position/orientation/velocity data with a 4-Hz update rate for the signal processing. The rms accuracy of the velocity was 0.1 m/s. In the signal processing, it was assumed that the flight path was straight, and linear resampling of the velocity values was calculated (from 4 Hz to 1 kHz). The grazing angle of the illumination from the DVB-T transmitter was around 3.5° for area No. 1 and around 1.8° for area No. 2 as presented in Fig. 4.

Area No. 1 marked in Fig. 4 was processed using the back-projection algorithm. The resulting passive SAR image is presented in Fig. 5 with its corresponding Google Earth map image—in Fig. 6. The passive SAR image of area No. 2 is presented in Fig. 7, together with its Google optical image

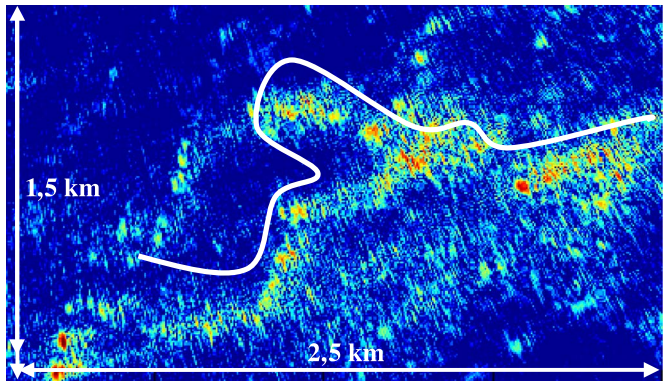

Fig. 7. Passive SAR image of area No. 2.

Fig. 8. Google optical image of area No. 1 (see Fig. 4).

(Fig. 8). Most of the targets, which are visible in the Google optical images, can be easily found in the passive SAR images. In these images (indicated in Figs. 5 and 6), the edges of the forest, as well as roads, private properties, and even a wind farm, are visible. Some of the targets, which are visible in the optical image, have no representation in their SAR counterparts and vice versa. This may be due to different reasons such as the differing time of acquisition of both images, among others. An additional reason might be the strong influence of shadowing between objects; the grazing angle of the illumination is close to 0°. For such low grazing angles of the DVB-T illumination, the terrain profile also has a strong influence on SAR imaging capability.

V. Conclusion

In this letter, the novel experimental results of a passive SAR imaging technique have been presented. The passive SAR imaging of ground targets utilizing the DVB-T illumination of opportunity was successfully demonstrated. Passive SAR radars provide certain advantages over the active SAR radar, such as a lack of emission of electromagnetic energy which results in silent operation. Moreover, the relatively low-frequency signals can penetrate foliage and other obstacles and be used for visualization of concealed targets.

However, the passive SAR radar is not free from drawbacks. As the illuminator of opportunity is placed at a relatively short distance from the ground, some areas can be shadowed. Another disadvantage is the complex signal processing, which

requires high computational power. The dynamic range is not sufficient in some cases, while strong direct echo leakage and strong echoes may mask weak stationary targets. This problem can be countered by applying appropriate signal processing methods, i.e., the adaptive removal of the direct echo or strong scatterers [17], [18], [23]. The authors strongly believe that this technology will be widely used in the near future.

REFERENCES

[1] C. Wiley, "Synthetic aperture radars," *IEEE Trans. Aerosp. Electron. Syst.*, vol. AES-21, no. 3, pp. 440–443, May 1985.

[2] W. G. Carrara, R. S. Goodman, and R. M. Majewski, *Spotlight Synthetic Aperture Radar*. Norwood, MA, USA: Artech House, 1995.

[3] K. Papathanassiou, F. Kugler, and I. Hajnsek, "Exploring the potential of POL-InSAR techniques at X-band: First results and experiments from TanDEM-X," in *Proc. IEEE 3rd Int. Asia-Pacific Conf. Synthetic Aperture Radar*, Seoul, South Korea, Sep. 26–30, 2011, pp. 1–2.

[4] H. D. Griffiths, C. J. Baker, J. Baubert, N. Kitchen, and M. Treagust, "Bistatic radar using satellite-borne illuminators," in *Proc. RADAR Conf.*, Edinburgh, U.K., Oct. 15–17, 2002, pp. 1–5.

[5] L. Maslikowski, P. Samczynski, M. Baczyk, P. Krysik, and K. Kulpa, "Passive bistatic SAR imaging—Challenges and limitations," *IEEE Aerosp. Electron. Syst. Mag.*, vol. 29, no. 7, pp. 23–29, Jul. 2014.

[6] M. Rodriguez-Cassola, S. V. Baumgartner, G. Krieger, and A. Moreira, "Bistatic TerraSAR-X/F-SAR spaceborne–airborne SAR experiment: Description, data processing, and results," *IEEE Trans. Geosci. Remote Sens.*, vol. 48, no. 2, pp. 781–794, Feb. 2010.

[7] G. Krieger, H. Fiedler, D. Hounam, and A. Moreira, "Analysis of system concepts for bi- and multi-static SAR missions," in *Proc. IEEE Int. Geosci. Remote Sens. Symp.*, Toulouse, France, Jul. 21–25, 2003, pp. 770–772.

[8] C. Prati, F. Rocca, D. Giancola, and A. Monti Guarnieri, "Passive geosynchronous SAR system reusing backscattered digital audio broadcasting signals," *IEEE Trans. Geosci. Remote Sens.*, vol. 36, no. 6, pp. 1973–1976, Nov. 1998.

[9] H. Ma, M. Antoniou, and M. Cherniakov, "Passive GNSS-based SAR resolution improvement using joint Galileo E5 signals," *IEEE Geosci. Remote Sens. Lett.*, vol. 12, no. 8, pp. 1640–1644, Aug. 2015.

[10] A. Evers and J. A. Jackson, "Experimental passive SAR imaging exploiting LTE, DVB, and DAB signals," in *Proc. IEEE Radar Conf.*, 2014, pp. 680–685.

[11] J. R. Gutiérrez Del Arroyo and J. A. Jackson, "WiMAX OFDM for passive SAR ground imaging," *IEEE Trans. Aerosp. Electron. Syst.*, vol. 49, no. 2, pp. 945–959, Apr. 2013.

[12] L. M. H. Ulander, P.-O. Frolind, A. Gustavsson, R. Ragnarsson, and G. Stenstrom, "VHF/UHF bistatic and passive SAR ground imaging," in *Proc. IEEE RadarCon*, May 10–15, 2015, pp. 0669–0673.

[13] L. Cazzani *et al.*, "A ground-based parasitic SAR experiment," *IEEE Trans. Geosci. Remote Sens.*, vol. 38, no. 5, pp. 2132–2141, Sep. 2000.

[14] A. D. Lazarov and T. P. Kostadinov, *Bistatic SAR/ISAR/FSR: Theory Algorithms and Program Implementation*. New York, NY, USA: Wiley, 2013.

[15] K. Kulpa, M. Malanowski, P. Samczynski, and B. Dawidowicz, "The concept of airborne passive radar," in *Proc. IEEE MRRS*, Aug. 25–27, 2011, pp. 267–270.

[16] D. Gromek, P. Samczynski, K. Kulpa, P. Krysik, and M. Malanowski, "Initial results of passive SAR imaging using a DVB-T based airborne radar receiver," in *Proc. IEEE 11th EuRAD*, Oct. 8–10, 2014, pp. 137–140.

[17] K. S. Kulpa and Z. Czekała, "Masking effect and its removal in PCL radar," *Proc. Inst. Elect. Eng. —Radar, Sonar Navigat.*, vol. 152, no. 3, pp. 174–178, Jun. 2005.

[18] K. Kulpa, "The CLEAN type algorithms for radar signal processing," in *Proc. IEEE MRRS*, Sep. 22–24, 2008, pp. 152–157.

[19] K. Kulpa, P. Samczynski, M. Malanowski, L. Maslikowski, and V. Kubica, "The use of CLEAN processing for passive SAR image creation," in *Proc. IEEE RADAR*, Apr. 29–May 3, 2013, pp. 1–6.

[20] O. Frey, C. Magnard, M. Rueegg, and E. Meier, "Non-linear SAR data processing by time-domain back-projection," in *Proc. IEEE 7th EUSAR*, Jun. 2–5, 2008, pp. 1–4.

[21] M. K. Bączyk, P. Samczyński, and K. Kulpa, "Passive ISAR imaging of air targets using DVB-T signals," in *Proc. IEEE Radar Conf.*, Cincinnati, OH, USA, May 19–23, 2014, pp. 502–506.

[22] D. Olivadese *et al.*, "Passive ISAR imaging of ships by using DVB-T signals," in *Proc. IEEE IET Int. Conf. Radar Syst.*, 2012, pp. 1–4.

[23] K. S. Kulpa, J. Misiurewicz, P. Samczyński, M. Smolarczyk, and M. Mordzonek, "SAR image enhancement by dominant scatterer removal," in *Proc. IEEE IET RADAR*, Edinburgh, U.K., Oct. 15–18, 2007, pp. 1–5.

[24] D. Gromek, P. Samczyński, K. Kulpa, J. Misiurewicz, and A. Gromek, "Analysis of range migration and Doppler history for an airborne passive bistatic SAR radar," in *Proc. IEEE 15th IRS*, Gdańsk, Poland, Jun. 2014, pp. 1–6.